

Generation of ‘Super-Ponderomotive’ Electrons due to a non-Wakefield interaction between a Laser Pulse and a Longitudinal Electric Field

A.P.L.Robinson,^{1,*} A.V.Arefiev,² and D.Neely¹

¹*Central Laser Facility, STFC Rutherford-Appleton Laboratory, Didcot, OX11 0QX, United Kingdom*

²*Institute for Fusion Studies, The University of Texas, Austin, Texas 78712, USA*

(Dated: March 4, 2013)

It is shown that electrons with momenta exceeding the ‘free electron’ limit of $m_e c a_0^2/2$ can be produced when a laser pulse and a longitudinal electric field interact with an electron via a non-wakefield mechanism. The mechanism consists of two stages: the reduction of the electron dephasing rate $\gamma - p_x/m_e c$ by an accelerating region of electric field and electron acceleration by the laser via the Lorentz force. This mechanism can, in principle, produce electrons that have longitudinal momenta that is a significant multiple of $m_e c a_0^2/2$. 2D PIC simulations of a relatively simple laser-plasma interaction indicate that the generation of super-ponderomotive electrons is strongly affected by this ‘anti-dephasing’ mechanism.

The production of highly energetic electrons in the interaction of ultra-intense laser pulses with plasmas [1] is an essential feature of laser-plasma physics that underpins a wide variety of topics ranging from wakefield acceleration [2] through to Fast Ignition inertial confinement fusion [3]. For certain topics the production of electrons with the highest energies possible is a matter of specific interest. Examples include laser-driven ion acceleration schemes based on energetic electrons [4] (e.g. Target Normal Sheath Acceleration and those closely related mechanisms), x-ray generation [5], strong field physics [6], and positron production in high Z targets [7].

The question as to how to reach high energies, and in particular how to exceed what might be termed the ‘free electron’ forward momentum limit of $m_e c a_0^2/2$ [8, 9] is therefore one of general interest. The wakefield scheme is one such route to producing high energies, although does not *directly* involve the laser field, and is not very well suited to producing high currents of energetic electrons (c.f. laser interactions with dense plasmas [10–14]). Mechanisms that can breach the ‘free electron’ limit and which directly involve the laser field seem to be more subtle, such as the ‘Direct Laser Acceleration’ scheme that takes place in the ion channel produced by transverse ponderomotive expulsion of electrons by the laser pulse. This was first analyzed by Pukhov et al. [15], and was more recently re-analyzed by Arefiev et al. [16]. In what follows we define the term ‘super-ponderomotive’ electron to mean an electron with forward momentum exceeding $m_e c a_0^2/2$.

In Ref. [16], a *general* mechanism of producing super-ponderomotive electrons was put forward. The interaction of an electron with a laser field in vacuum will have an integral of motion of the form $\gamma - p_x/m_e c = R$ [8, 9]. It is also the case that $\gamma - p_x/m_e c$ is the dephasing rate of the electron, and the ‘free electron’ momentum limit arises from $R = 1$ in the absence of any fields apart from the laser field. Arefiev et al. showed that, in the *specific* case of the ion channel, the transverse electro-

static field in the ion channel can reduce the dephasing rate, and thus super-ponderomotive electrons can be produced. However there is no *a priori* reason why only a transverse electric field can reduce R below unity.

In this Letter we show that this very general mechanism extends to the longitudinal electric field as well, i.e. collective electric field in the direction of laser propagation. Longitudinal electric fields are also naturally established in laser-plasma interactions by ponderomotive displacement of electrons, so they are a clear ‘next candidate’ for extra fields that could reduce the dephasing rate. We show that super-ponderomotive energies can result from electron interactions with spikes of relatively weak longitudinal electrostatic field. In contrast with the wakefield acceleration, the axial acceleration in this case is insignificant in terms of the direct energy gain. Instead, the role of the longitudinal field is a reduction of dephasing that subsequently allows for an extended interaction with the laser field and leads to a significant energy enhancement. The strongest increase in energy occurs if the interaction with the longitudinal field is terminated as the electron passes through a zero in the vector potential of the laser field. This indicates that there are certain parallels with other relativistic laser-plasma phenomena where vector potential zeroes are critical [17–19]. This mechanism can work in a region of underdense to near-critical plasma formed in front of a dense target. Therefore, it may be the case that the mechanism is partly responsible for the production of highly energetic electrons in current and extant experiments. To show that this mechanism can naturally occur in laser-target interactions, we also present a 2D particle-in-cell (PIC) simulation of an extended underdense target irradiated by an intense laser beam. We demonstrate that a self-consistently generated quasi-static longitudinal electric field at the edge of the plasma significantly reduces the dephasing rate and enables production of super-ponderomotive electrons by the laser beam.

Consider the dynamics of a single electron in an essen-

tially 1D configuration in which it interacts with a plane electromagnetic wave described by the vector potential,

$$\mathbf{A} = [0, 0, A] = [0, 0, A_0 \cos(\omega_L \tau)], \quad (1)$$

where $\tau = t - x/c$, and ω_L is the frequency of the field. The electric and magnetic fields are related to the vector potential via $\mathbf{E} = -\partial_t \mathbf{A}$ and $\mathbf{B} = \nabla \times \mathbf{A}$, so the electric field of this wave is polarized in the z -direction. We also consider the case where a longitudinal electric field, E_x , is present. The equations of motion of the electron that need to be considered are:

$$\frac{dp_x}{dt} = -eE_x + ev_z B_y, \quad (2)$$

$$\frac{dp_y}{dt} = 0, \quad (3)$$

$$\frac{dp_z}{dt} = -eE_z - ev_x B_y, \quad (4)$$

$$\frac{d\gamma}{dt} = -\frac{ev_z E_z}{m_e c^2} - \frac{ev_x E_x}{m_e c^2} \quad (5)$$

From the definition of τ ($\tau \equiv t - x/c$), one can differentiate to obtain,

$$\frac{d\tau}{dt} = 1 - \frac{v_x}{c}, \quad (6)$$

and this can then be used to write the field components as $E_z = -\partial_\tau A$, $B_y = (1/c)\partial_\tau A$. These can then be used to obtain, $p_z = eA$, from Eq. 4, which is one of the key integrals of motion. In the absence of E_x , another integral of motion is obtained from Eqs 2 and 5, namely $\gamma - p_x/m_e c = 1$ (assuming that the electron is initially at rest). Using this, one obtains $p_x = e^2 A^2 / 2m_e c$ in the $E_x = 0$ case (i.e. the ‘free electron’ case). If, however, $E_x = -E$ (where E is a positive constant over some region) then we instead have,

$$\frac{d}{d\tau} \left(\gamma - \frac{p_x}{m_e c} \right) = -\frac{eE}{m_e c}, \quad (7)$$

and from this we can see that $\gamma - p_x/m_e c < 1$. We can now re-write Eq. 2 as,

$$\frac{dp_x}{dt} = \frac{1}{R} \frac{e^2 A}{m_e c} \frac{dA}{dt} + eE, \quad (8)$$

where

$$R = \gamma - \frac{p_x}{m_e c} = 1 - \frac{eE}{m_e c} \int d\tau. \quad (9)$$

From Eqs. 8 and 9 one can see that the effect of the accelerating electric field will not only be direct acceleration of the electron (similar to wakefield acceleration),

but it will also be a reduction of the dephasing rate R . As a result, the electron will gain additional energy from the laser field above that obtained in the free electron case, i.e. it can produce super-ponderomotive electrons. Equation 8 also emphasizes that the ‘ $\mathbf{j} \times \mathbf{B}$ ’ force is not entirely separated from the longitudinal electric force, as the two are linked through the dephasing rate.

If the electric field has a limited spatial extent, then after passing through this spike one will have $E_x = 0$, but it will still be the case that $\gamma - p_x/m_e c = R$, and Eq. 8 can then be directly integrated to give,

$$p_x = p_x^* + \frac{m_e c}{2} \frac{a^2 - a^{*2}}{R}, \quad (10)$$

where we have normalized the vector potential via $a = eA/m_e c$, and where p_x^* and a^* are the longitudinal momentum and normalized vector potential immediately after the interaction with the spike in the electric field. It is clear that the largest effect will be obtained if the dephasing rate R is significantly reduced and the region of interaction with E_x terminates close to a zero in the vector potential ($a^* \ll a_0$). At $a^* = 0$, we have $p_z = 0$ and we immediately find that the reduced dephasing rate in this case is given by

$$R = \gamma - p_x^*/m_e c = \sqrt{(p_x^*/m_e c)^2 + 1} - p_x^*/m_e c. \quad (11)$$

To significantly decrease the dephasing rate ($R \leq 0.5$), the longitudinal momentum following the interaction has to be relativistic. Specifically, assuming that $p_x^*/m_e c \gg 1$, we find directly from Eqs. (11) and (10) that

$$R \approx m_e c / 2p_x^* \quad (12)$$

and

$$p_x \approx p_x^* (1 + a^2). \quad (13)$$

Therefore, the axial momentum can be enhanced by as much as a factor of $2p_x^*/m_e c$ compared to the ‘free electron’ limit. Equation (13) confirms that the longitudinal momentum can be significantly enhanced even if the change in the longitudinal momentum during the interaction with the static field is relatively small ($a_0^2 \gg p_x^*/m_e c \gg 1$).

To estimate the amplitude of the static field required to reduce the dephasing rate, $R = \gamma - p_x/m_e c$, well below 1, we again use the assumption of a region of uniform electric field. Making use of Eqs 6 and 7 we have $d\tau/dt = R/\gamma$. From this the two key equations to consider are Eq.8 and,

$$\frac{dR}{dt} = -\frac{eE}{m_e c} \frac{R}{R + \frac{p_x}{m_e c}}. \quad (14)$$

From Eq.14 we can see that at the zeros in the vector potential ($p_x \approx 0$) we can achieve a rapid fall in

R , i.e. $dR/dt = -eE/m_e c$. At the peaks of the laser field ($p_x \approx e^2 A^2 / 2m_e c$) the reduction in dephasing will be much slower, i.e. $dR/dt \approx -(eE/m_e c)(2R/a_0^2)$. One therefore expects, in general, for the largest drops in dephasing to occur around zeroes in the vector potential. To significantly decrease the dephasing rate ($R \leq 0.5$) in a single spike around a zero in the vector potential, one would estimate $\delta t \approx 1/(a_0 \omega_L)$ which implies $E \approx E_L/2\pi$, where E_L is the amplitude of the laser field. With a more extended electric field, the actual field magnitude required will be significantly less.

The insights gained from this analysis can be verified by direct numerical integration of Eqs 2–4 along with $dx/dt = p_x/\gamma m_e$ for particular laser fields and choices of E_x . Here we show the result of a calculation performed with a laser field defined (in terms of normalized vector potential) by,

$$a_z = a_0 \cos(\omega_L \tau) \exp \left[\frac{-(x - ct - x_0)^2}{2c^2 t_L^2} \right], \quad (15)$$

where $a_0 = 10$, $\lambda = 1\mu\text{m}$, $x_0 = 6ct_L$, and $t_L = 40$ fs. The electron is initially at rest at the origin. A constant longitudinal electric field had a magnitude equal to $E_x = -0.1E_L$ over the region $142\mu\text{m} \leq x \leq 147\mu\text{m}$. The E_x component is zero at all other points. The change in the electrostatic potential across this region is approximately 16 MeV, which would result in accelerating the electron to $p_x/m_e c \approx 31$ without the laser field.

The results of this calculation shown in Fig. 1 demonstrate that the effect of the longitudinal field is to drive the electron onto a strongly super-ponderomotive trajectory. It is evident from the plot of a at the electron location that the interaction with the longitudinal field lasts less than a single oscillation of the laser field (the red segment of the curve). The immediate effect of the axial electric field in this specific case is negative, as the axial momentum decreases during the interaction compared to the axial momentum calculated with $E_x = 0$. However, the interaction also leads to a considerable drop in $\gamma - p_x/m_e c$ and it terminates close to a zero in the vector potential. As a result, a subsequent interaction with the laser field leads to a significant longitudinal acceleration, with the peak momentum in the excess of $1000 m_e c$. This result is consistent with Eq. (10) since $p_x^*/m_e c \approx 27.52$, $R \approx 0.042$, $a_0 = 10$, and $a^*/a_0 \approx 0.116$.

Note that if the longitudinal electric field does not accelerate the electrons in the direction of the laser pulse, then the effect of the longitudinal electric field will be instead to reduce the electron momentum. In actual laser-plasma interactions, there is a considerable degree of complexity, and this means that a full assessment of this anti-dephasing mechanism requires a fuller model for a more complete assessment.

Nonetheless the insights gained from studying single electron motion are of great benefit when the results of

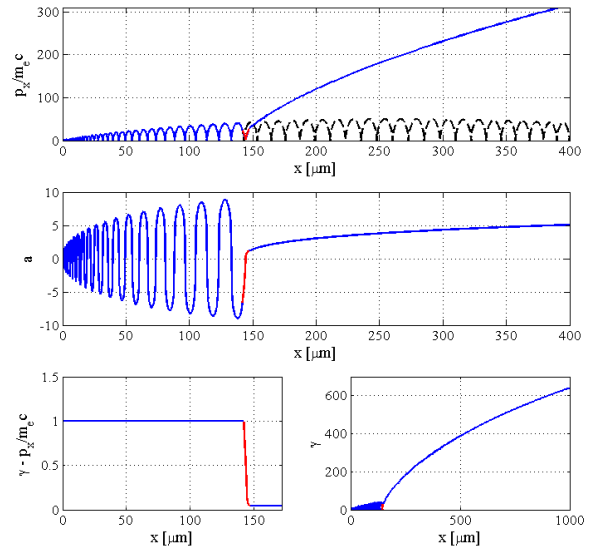


FIG. 1. Results of the case A calculation for single electron motion (red line). Region of accelerating E_x located over $142 \leq x \leq 147\mu\text{m}$. Plot shows (a) longitudinal component of electron momentum, (b) vector potential at the electron location; (c) the dephasing rate, $\gamma - p_x/m_e c$, and (d) the relativistic γ -factor. Black line in upper panel is the same plot for the case without E_x .

2D Particle-In-Cell (PIC) simulations are analyzed in detail. A 2D PIC simulation was carried out using the Plasma Simulation Code (PSC), in which a laser pulse was normally incident significantly underdense hydrogenic plasma at a density of $8 \times 10^{25} \text{m}^{-3}$. The length and width of the slab being $200\mu\text{m}$ and $160\mu\text{m}$ respectively, and the simulation domain was $300\mu\text{m}$ by $200\mu\text{m}$. The laser pulse had an a_0 of 10, a FWHM width of $8\mu\text{m}$, and a pulse duration of 500 fs. Denoting the two axes of the simulation domain as x (laser direction) and y , the electric field of the laser pulse was polarized in the z direction.

This pulse is significantly longer than the characteristic time of electron response in the plasma, so that the laser eventually creates a quasistatic channel shown in Fig. 2. The channel has a coaxial structure with a positively charged center and negatively charged walls. During the formation of the channel, the electrons from inside the channel are expelled radially by ponderomotive pressure, which causes charge separation. The resulting radial electric field counteracts the expelling force, allowing the electrons to remain in an equilibrium bunched on the periphery of the laser beam. Such channels and the corresponding transverse electric field are routinely observed in simulations of laser interactions with underdense plasmas [20–23]. However, the fact that such a coaxial structure would also produce a quasistatic axial

electric field at the channel entrance (see Fig. 2) has been underappreciated.

In order to examine the role played by the axial field, we have performed a search on the electron particle data for super-ponderomotive electrons for which the dephasing rate satisfied $\gamma - p_x/m_e c < 0.05$ and $x < 50 \mu\text{m}$ at least at some point during the electron trajectory. In Fig. 2 we show a trajectory, axial momentum, and dephasing for just one such electron. Near the front of the slab, there is a region with a strong quasi-static negative E_x . Clearly, the electron interaction with this field (shown on all plots with a red segment) launches the electron onto a super-ponderomotive trajectory (the subsequent acceleration is shown with a light-blue curve). There is virtually no self-focusing of the laser pulse in this region ($a_0 \approx 10$), so the free-electron limit for γ is 50. The electron however achieves a peak γ of nearly 150, which exceeds the free-electron limit by a factor of three. The acceleration is preceded by a massive drop in the dephasing rate that occurs during the interaction with E_x when the electron moving against the laser beam is turned around and pushed forward. The time evolution of the axial momentum further emphasizes that this is a two-stage process, since no significant axial acceleration occurs directly during the interaction with the axial field.

It must be pointed out that the electric field of the laser is polarized out of the plane of the simulation domain, which eliminates forced driving of betatron oscillations [15] as a possible explanation for the observed significant energy gain. Moreover, we observe no amplification of the transverse oscillations across the channel, which indicates that the observed effect is not related to the parametric amplification of betatron oscillations [16]. Figure 2 clearly shows that this event is quite prompt, so the underlying mechanism must be able to produce the observed behavior without any gradual build-up. The reduction of dephasing by acceleration in the longitudinal electric field clearly satisfies this key criterion.

Later on it can be seen that there is a decline in the electron momentum. This illustrates the concern, stated earlier, that the collective fields can also act to increase the dephasing rate. Note that in this simulation there is no dense foil which will interrupt the acceleration process. We have therefore made no attempt to determine the optimal conditions for exploiting this anti-dephasing mechanism, and this is matter for future work as these conditions will be highly dependent on the specifics of the laser and target parameters.

In this Letter we have shown that, according to the single electron equations of motion, electrons can be accelerated to momenta in excess of $m_e c a_0^2/2$ by an ‘anti-dephasing’ mechanism in which a brief acceleration by a longitudinal electric field that is simultaneously present with the laser pulse reduces $\gamma - p_x/m_e c$ significantly below unity. This was verified by direct numerical integration of the equations of motion and then the ef-

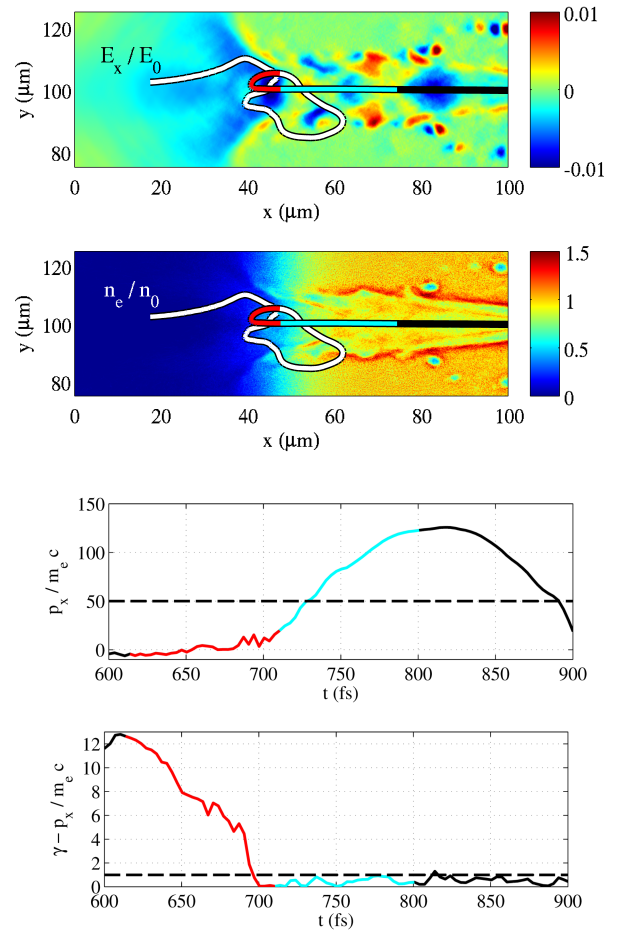


FIG. 2. Snapshots of time-averaged axial electric field, electron density, and time evolution of the electron axial momentum and the dephasing from a 2D PIC simulation.

fect was confirmed in a fully self-consistent simulation of laser-plasma interaction (laser pulse propagating in under-dense plasma). This therefore shows that the anti-dephasing mechanism both exists and can play a very important role in the production of super-ponderomotive electrons in laser-plasma interactions. This mechanism is complimentary to the mechanism of the parametric amplification of betatron oscillations, so that the combination of the two can produce super-ponderomotive electrons with energies exceeding what is predicted here and in Ref. [16]. The work presented here also shows that one cannot simply split electron motion into an independent ‘wakefield-like’ component and a ‘free electron like’ component, when in fact the anti-dephasing mechanism is due to a subtle interaction between the two.

APLR is grateful for computing resources provided by STFC’s e-Science facility. AVA acknowledges the Texas Advanced Computing Center at The University of Texas at Austin for providing HPC resources. AVA was supported by National Nuclear Security Administration

Contract No. DE-FC52-08NA28512, U.S. Department of Energy Contract No. DE-FG02-04ER54742, and Sandia National Laboratory Contract No. PO 990947.

* alex.robinson@stfc.ac.uk

- [1] S. C. Wilks, W. L. Kruer, M. Tabak, and A. B. Langdon, *Phys. Rev. Lett.* **69**, 1383 (1992).
- [2] S. P. D. Mangles *et al.*, *Nature* **431**, 535 (2004).
- [3] M. Tabak *et al.*, *Phys. Plasmas* **1**, 1626 (1994).
- [4] M. Roth *et al.*, *Plasma Phys. Control. Fusion* **44**, B99 (2002).
- [5] S. Kneip *et al.*, *Proc. SPIE* **7359**, 73590T (2009).
- [6] C. P. Ridgers *et al.*, *Phys. Rev. Lett.* **108**, 165006 (2012).
- [7] H. Chen *et al.*, *Phys. Rev. Lett.* **105**, 015003 (2010).
- [8] T.J.M. Boyd and J.J. Sanderson, *The Physics of Plasmas* (Cambridge University Press, 2003).
- [9] A. Pukhov, *Rep. Prog. Phys.* **66**, 47 (2003).
- [10] S. C. Wilks and W. L. Kruer, *IEEE J. Quant. Elec.* **33**, 1954 (1997).
- [11] B. Chrisman, Y. Sentoku, and A. J. Kemp, *Phys. Plasmas* **15**, 056309 (2008).
- [12] H. Habara *et al.*, *Phys. Rev. Lett.* **97**, 095004 (2006).
- [13] W. Yu *et al.*, *Phys. Rev. Lett.* **85**, 570 (2000).
- [14] S. A. Gaillard *et al.*, *Phys. Plasmas* **18**, 056710 (2011).
- [15] A. Pukhov, Z.-M. Sheng, and J. Meyer-ter-Vehn, *Phys. Plasmas* **6**, 2847 (1999).
- [16] A. V. Arefiev *et al.*, *Phys. Rev. Lett.* **108**, 145004 (2012).
- [17] T. Baeva, S. Gordienko, A. P. L. Robinson, and P. A. Norreys, *Phys. Plasmas* **18**, 056702 (2011).
- [18] T. Baeva, S. Gordienko, and A. Pukhov, *Phys. Rev. E* **74**, 046404 (2006).
- [19] T. Baeva, S. Gordienko, and A. Pukhov, *Phys. Rev. E* **74**, 065401(R) (2006).
- [20] Y. Sentoku, W. Kruer, M. Matsuoka, A. Pukhov, *Fusion Science and Technology* **49**, 278 (2006).
- [21] G. Li *et al.*, *Phys. Rev. Lett.* **100**, 125002 (2008).
- [22] G. Sarri *et al.*, *Phys. Plasmas* **17**, 113303 (2010).
- [23] A. Friou, E. Lefebvre, and L. Gremillet, *Phys. Plasmas* **19**, 022704 (2012).